Numerical evidence of universal scaling for the scalar variance spectrum in forced homogeneous turbulence

Jean-Baptiste Lagaert, Guillaume Balarac, Georges-Henri Cottet

Numerical evidence of universal scaling for the scalar variance spectrum in forced homogeneous turbulence

J.-B. Lagaert[1,2], G. Balarac[1] and G.-H. Cottet[2]

[1] Grenoble-INP / CNRS / UJF-Grenoble 1, LEGI UMR 5519, Grenoble, F-38041, France

[2] Grenoble-INP / CNRS / UJF-Grenoble 1, LJK UMR 5224, Grenoble, F-38041, France

(Dated: 28 February 2013)

In this letter, the spectrum of high Schmidt number passive scalar in forced homogeneous isotropic turbulence is studied through direct numerical simulations. A hybrid spectral-particle method[1] is used with a finer resolution of the scalar than of the momentum and large time-steps. This approach enables to perform a systematic analysis over a wide range of Schmidt numbers. Our results recover the theoretical scaling for the variance scalar spectrum, and its relationship with the value of the Schmidt number, for large, intermediate and small scales. The influence of the form of the scalar forcing is also discussed.

The prediction of the dynamics of a scalar advected by a turbulent flow is an important challenge in many applications. The scalar field can be used to describe the temperature field or the concentration of chemical species, for example. For a passive scalar, Z, the transport equation is an advection-diffusion equation,

$$\frac{\partial Z}{\partial t} + \vec{u} \cdot \vec{\nabla} Z = \vec{\nabla} \cdot \left(\kappa \vec{\nabla} Z \right) \tag{1}$$

where κ is the molecular scalar diffusivity and $\vec{u}$ the turbulent velocity field. The phenomenology of passive scalar diffusion depends on the molecular Schmidt numbers, the viscosity-to-diffusivity ratio, $Sc = \nu/\kappa$. For high Schmidt number, similar to the Kolmogorov scale, η_K, which describes the smallest scale of turbulence motions beyond which dissipation dominates, the Batchelor scale, η_B, describes the smallest length scale of the scalar fluctuations that can exist before being dominated by molecular diffusion. This scale is smaller than the Kolmogorov scale. This means that scalar dynamics can occur at scales smaller than the smallest velocity eddy. An important theoretical result is the influence of the Schmidt number on the behavior of the scalar variance spectrum[2]. For a Schmidt number larger than one, Batchelor[3] explained that the classical Corrsin-Obukhov cascade associated with a $k^{-5/3}$ law (where k is the wave number) for the scalar variance spectrum[4,5] is followed by a viscous-convective range with a k^{-1} power law. This viscous-convective range is followed by the dissipation range, where various theoretical scalings have been proposed for the spectrum[3,6]. However, some recent numerical results[7] seem to suggest that the k^{-1} law exists even for Schmidt numbers smaller than one (see Fig. 1 in Donzis et al.[7]). Moreover, the $k^{-5/3}$ law appears only for very high Reynolds numbers (in Fig. 3 from Donzis et al.[7], this range exists for $R_\lambda \approx 650$ but not for $R_\lambda \approx 140$, with R_λ the Taylor-scale Reynolds number). These results[7] were obtained by using a uniform mean scalar gradient to maintain scalar variance[8]. The objective of this letter is to compare DNS results with theoretical predictions for small, intermediate and large scales, over a wide range of Schmidt numbers, and to show the influence of the scalar forcing on this behavior.

For DNS of scalar mixing at high Schmidt number, the dependence of the Batchelor scale on the Schmidt number suggests that the prediction of scalar dynamics for high Schmidt numbers is more demanding in terms of spatial resolution than the prediction of momentum. In Cottet et al[9], a remeshed particle method with different grid resolutions for vorticity particles and scalar particles, was proposed. In Lagaert et al.[1], this method was extended to

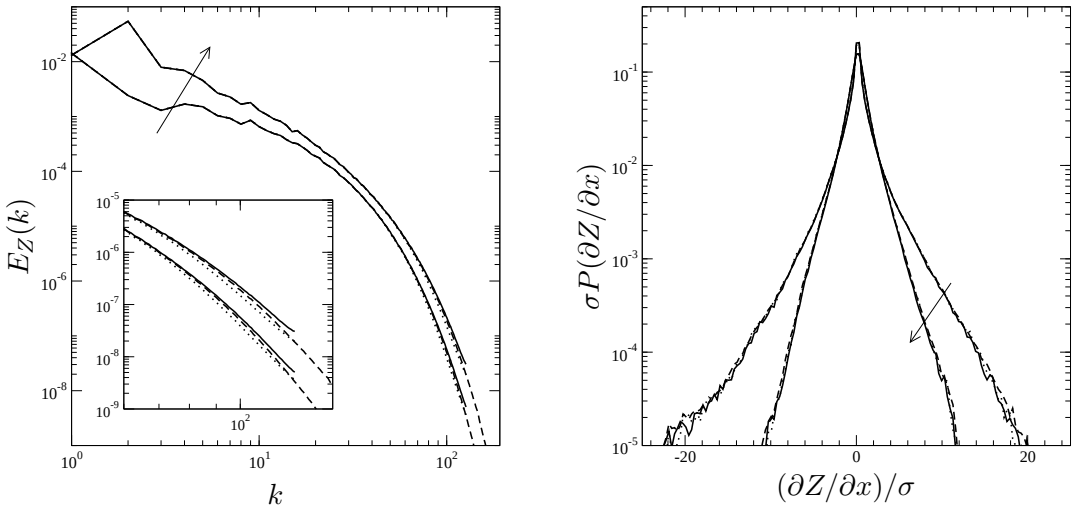

FIG. 1. Comparison for two different times of the scalar spectra (left) and probability density functions (PDF) of the scalar gradient (right) obtain with a full spectral method on 256^3 grid points (solid lines), and with our hybrid method for different resolutions: 256^3 (dotted lines) and 384^3 (dashed lines) grid points. The arrow shows the direction of increasing time.

couple a full spectral Navier-Stokes solver with a high order particle method[10] for the scalar. The principle of remeshed particle method for the advection of a given quantity is to concentrate this quantity on a set of particles, to follow these particles with the advection field and to remesh them on a regular grid through interpolation[11]. In the context of the advection of a vorticity field to solve the incompressible Navier-Stokes equation in vorticity form, these methods have been validated against spectral or finite-difference methods and applied in bluff body flows[12–15], in homogeneous decaying turbulence[16] and in vortex flows[17,18]. Concerning scalar advection they have been used in the context of level set methods[10,19,20]. In Magni et *al.*[10] the value of the time-step used to advect particles and the impact of the interpolation kernel used to remesh particles are analyzed from the stability point of view. In the present paper we use a fifth order interpolation kernel derived in Bergdorf et *al.*[20], and following Magni et *al.*[10], our time-step is given by

$$\Delta t^z = (2 \max |\nabla \vec{u}|)^{-1}. \tag{2}$$

Note that $(\max |\nabla \vec{u}|)^{-1}$ is the relevant time scale for the advection of a quantity with a velocity $\vec{u}$. In practice, with Schmidt numbers larger than one, we have observed that the

diffusive time-scales were of the same order or bigger. This time-step value is therefore also consistent with the time-scales that need to be resolved to ensure accurate results for the advection-diffusion equations that we had to deal with.

We give in Figure 1 comparisons of the results obtained for decaying turbulence by solving the scalar equation by a particle method and by a pseudo-spectral method. In both cases the Navier-Stokes equations were solved by a pseudo-spectral method. The Taylor-scale Reynolds and Schmidt numbers were chosen equal to 130 and 0.7 respectively. The initial velocity is obtained by reaching a steady-state with the Alvelius forcing term[21]. The scalar is initialized with the procedure described by Esweresan and Pope[22]. For this particular case ($R_\lambda = 130$ and $Sc = 0.7$), the pseudo-spectral method was fully resolved with $N = 256$ modes. We show in the left (resp. right) picture the spectra (resp. the PDF of the scalar derivative) at two different times and for two different grid-sizes for the particle method. From these results one may conclude that spectral accuracy in the dissipative range of the scalar can be obtained with a particle resolution roughly equal to 1.5 times the spectral resolution. Based on a reference spectral resolution given with $\eta_B/\Delta x^z = 1.5/\pi \simeq 0.48$ (to insure $k_{\max}\eta_B \simeq 1.5$), this would correspond to a particle resolution given by $\eta_B/\Delta x^z \simeq 0.72$. In the numerical experiments recorded in Table I, we used values of $\eta_B/\Delta x^z$ ranging between 0.56 and 1.08, depending on the runs. The analysis of the spectra in the dissipative range that we show later on Fig. 4 (right) shows that the dissipative scales, although slightly under-resolved for some of the cases that we ran, allow to conclude on the universal scaling law.

The idea of using particle methods and different grid-sizes for DNS of turbulent transport[1,9,10] relies on the observation already mentioned that scalar significant scales for the scalar can exist beyond the Kolmogorov scales. The ratio between grid-sizes for the momentum and the scalar is determined by the ratio between the Kolmogorov and Batchelor scales, $\eta_K/\eta_B = Sc^{1/2}$. The extension of particle methods in combination with a spectral method for the Navier-Stokes to this case is straightforward if the ratio between the (fine) scalar grid-size and the (coarse) momentum grid size is an integer : the velocity is computed in the spectral space then padded with zeros to obtain modes corresponding to the finer grid-size used for the particle methods, then transformed back in the physical space on the fine grid. This velocity field is then interpolated onto particle locations to obtain particle velocities. Since, from Eq. (2), the time-step for the particle methods is only on the underlying velocity,

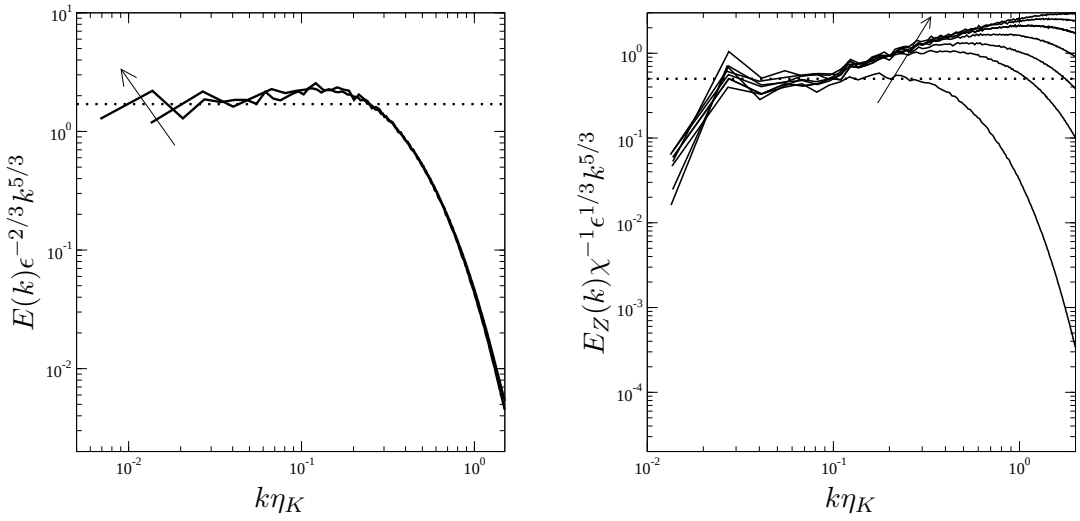

FIG. 2. Left picture: Energy spectra for both Reynolds numbers, $R_\lambda \approx 130$ and $R_\lambda \approx 210$. The spectra are compensated by the Kolmogorov scaling and the dotted line is for $C_K = 1.8$. The arrow shows the direction of increasing Reynolds numbers. Right picture: Scalar variance spectra for $R_\lambda \approx 130$. The spectra are compensated by the scaling proposed by Corrsin-Obukov and the dotted line is for $C_{CO} = 0.5$. The arrow shows the direction of increasing Schmidt numbers.

it does not depend on the scalar resolution and thus on the Schmidt number. This can result on substantial computational savings compared e.g. to the hybrid spectral/finite-difference strategy of Gotoh et al.[23] in which the finite-difference method, like the spectral method, requires to satisfy a CFL condition corresponding to the scalar grid-size. To illustrate this feature, Table I indicates the time-step values used in our different simulations. Our simulations ran on 512 to 8192 cores of an IBM Blue Gene-P cluster with a strong scalability of 85% for the biggest configuration. By strong scalability, we mean the ratio between the theoretical time on 8192 computed from an extrapolation from the computational cost on 512 cores (*i.e.* divided by 16) and the actual computational cost on 8192 cores. For the biggest configuration, with a resolution of 256^3 grid points for the momentum and 3064^3 points for the scalar, running on 8192 cores, the time-step for the spectral-particle method given by Eq. (2) was equal to 0.08 and the CPU time was 76s. For the same resolutions a fully spectral method would have required for the scalar advection a time-step value of 0.001 and, from extrapolation of the CPU time we obtained in a simulation using 512^3 modes, the CPU time to reach $t = 0.08$ would have been roughly equal to 5700s.

R_λ	N^u	$\eta_K/\Delta x^u$	Δt^u	Sc	N^z	$\eta_B/\Delta x^z$	Δt^z	Δt^z_{spec}
130	256	0.55	1.2e^{-2}	0.7	512	-	8.6e^{-2}	6e^{-3}
				4	1024	1.08		3e^{-3}
				8	1024	0.78		3e^{-3}
				16	1536	0.83		2e^{-3}
				32	1536	0.59		2e^{-3}
				64	2048	0.56		1.5e^{-3}
				128	3064	0.57		1e^{-3}
210	512	0.57	3e^{-3}	0.7	770	1.03	2e^{-2}	2e^{-3}
				4	1024	0.56		1.5e^{-3}

TABLE I. Setup of simulations performed. N^u, Δx^u and Δt^u are the number of points in each direction, the spatial step and the time step, respectively, used to solve the Navier-Stokes equation with a pseudo-spectral solver. N^z, Δx^z and Δt^z are the number of points in each direction, the spatial step and the time step, respectively, used to solve the scalar transport equation with the particle method. Δt^z_{spec} is the time step which would be needed if a pseudo-spectral method was used for the same number of scalar grid points.

Based on this hybrid solver, various simulations have been performed in the context of forced homogenous isotropic turbulence (HIT), in a 3D periodic box with a length 2π. The forcing scheme used to obtain a statistical steady flow follows the one proposed by Alvelius[21]. To achieve a steady state for the scalar, a forcing scheme is also applied to low wave number modes in Fourier space, similarly to velocity forcing[24]. Two Taylor-scale Reynolds number, R_λ, are considered, 130 and 210, using a resolution of 256^3 and 512^3 grid points, respectively. Figure 2 (left) shows the compensated spectrum for the kinetic energy, with ϵ, the mean energy dissipation rate. For the scalar field, the mesh resolution is increased with the Schmidt number[25]. Simulation details are given in Table I. Figure 3 illustrates the scales separation between the Kolmogorov and Batchelor scales for the highest Schmidt number case, $Sc = 128$.

The behaviors of the scalar variance spectrum are studied at large, intermediate and small scales from this DNS database and compared with theoretical predictions. First,

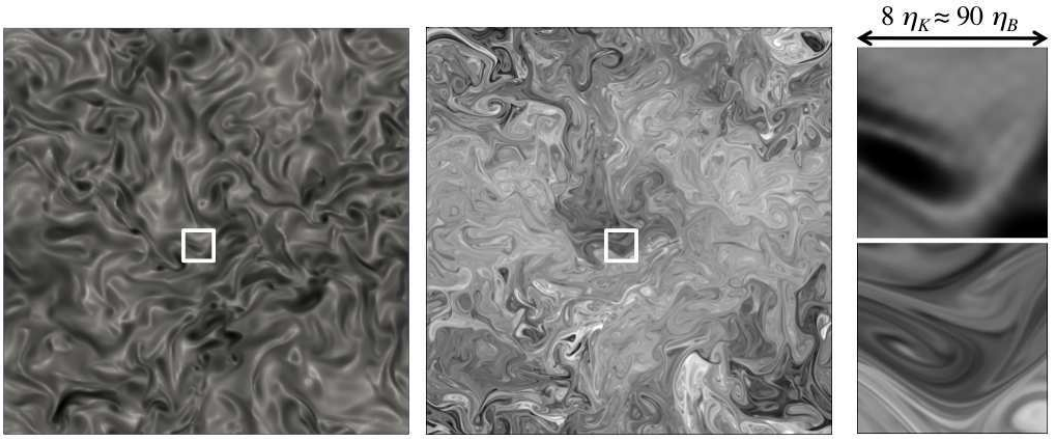

FIG. 3. $x - y$ plan colored by the vorticity magnitude (left, dark regions are for the highest vorticity values) and by the passive scalar (middle, dark regions are for the highest scalar values) for $R_\lambda \approx 130$ and $Sc = 128$. The zooms (right) correspond to the white box with a length of $8\eta_K$ for the vorticity magnitude (top) and the scalar (bottom).

at the scales beyond the forcing peak, the classical Corrsin-Obukhov cascade is expected to characterize the inertial-convective range. Similarly to the inertial range of the kinetic energy spectrum, it is expected that this cascade follows a $k^{-5/3}$ law[4,5]. Figure 2 (right) shows the scalar spectra for various Schmidt numbers, compensated by the Corrsin-Obukhov scaling, with χ the mean scalar dissipation rate. As expected, the results show a inertial-convective range independent of the Schmidt number. The Corrsin-Obukhov constant, C_{CO}, is found approximately around 0.5. This result is consistent with previous results[8,26]. The $k^{-5/3}$ range of the scalar spectrum is found more clearly than the $k^{-5/3}$ range of the energy spectrum. Indeed, the scalar spectrum exponent is known to tend to the $-5/3$ value more rapidly than the energy spectrum exponent[27,28]. Note that the end of the inertial-convective range appears around $k\eta_K \approx 0.1$ (which is roughly the Taylor scale) independently of the Schmidt number.

Beyond this range, for Schmidt numbers larger than one, Batchelor[3] explained the development of the viscous-convective range with a k^{-1} law. This scaling is due to the velocity small scales strain effect on the scalar field. Figure 4 shows the scalar spectra for various Schmidt numbers, compensated by the Batchelor's scaling. For clarity, the results are shown with wavenumbers multiplied by the Kolmogorov scale (Fig. 4 left) or by the Batchelor scale

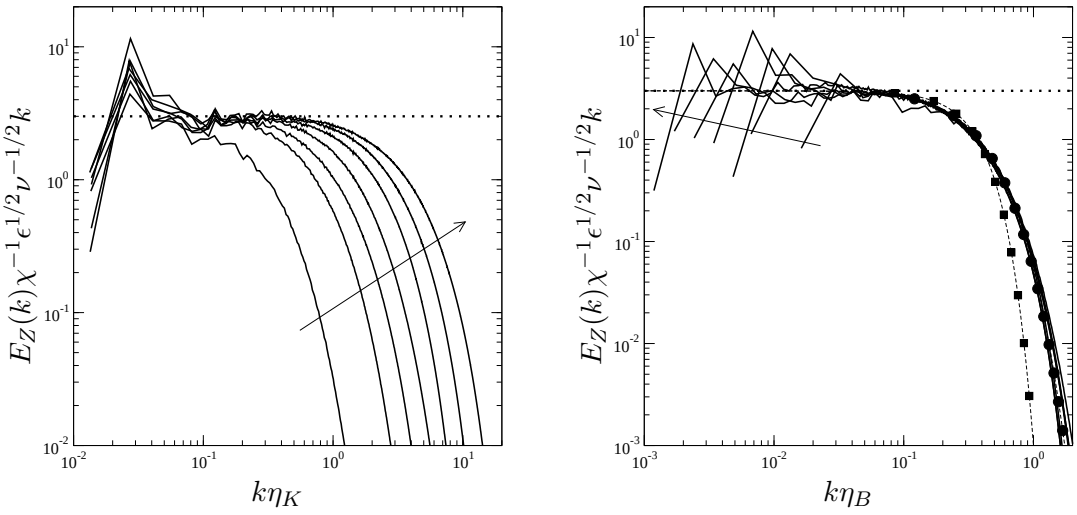

FIG. 4. Scalar variance spectra for $R_\lambda \approx 130$. The spectra are compensated by the scaling proposed by Batchelor for Schmidt number higher than one, and the dotted line is for $C_B = 3$. The arrow shows the direction of increasing Schmidt numbers. For a sake of clarity, the results are shown with wavenumbers multiplied by the Kolmogorov scale (left) and by the Batchelor scale (right). For the dissipative region, the circles show the law proposed by Kraichnan and the squares show the law proposed by Batchelor (right).

(Fig. 4 right). From our numerical results, the -1 power law starts from $k\eta_K \approx 0.1$, after the inertial-convective range, and this viscous-convective range grows with the Schmidt number (Fig. 4 left). The Batchelor constant, C_B, if found around 3. This value is in the range given in previous numerical or analytical works[7,29,30] and larger than the theoretical value of 2 initially proposed by Batchelor. The form of the scalar variance spectrum in the dissipation range (following the viscous-convective range) is also studied (Fig. 4 right). Two distinct theoretical behaviors have been proposed by Batchelor[3] and Kraichnan[6], respectively. Note that the distinction between these behaviors has some practical implications on our understanding of energy transfer between ocean and atmosphere[31]. Although, as mentioned earlier, some of our runs were slightly over dissipative in this range, our DNS results, clearly show a good agreement with the Kraichnan form, as already established in various previous works[7,31,32]. Note that, Donzis et al.[7] observed that even for Schmidt number smaller than 1, the scalar spectra collapse in the dissipative range when they are normalized by Batchelor variables. The same trend is found with our numerical results for

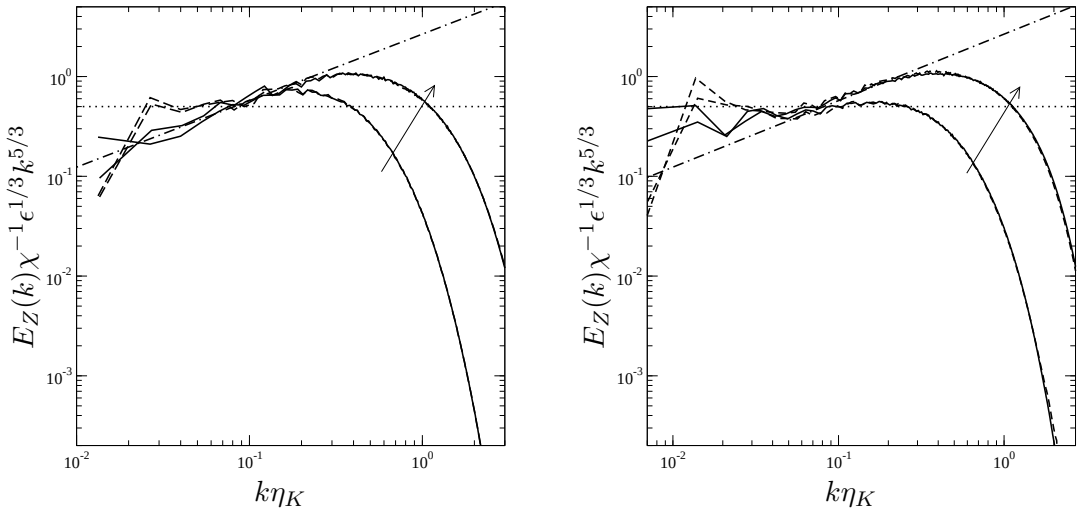

FIG. 5. Scalar variance spectra for two Schmidt number, $Sc = 0.7$ and $Sc = 4$ for $R_\lambda \approx 130$ (left) and $R_\lambda \approx 210$ (right). The spectra are compensated by the scaling proposed by Corrsin-Obukov and the dotted line is for $C_{CO} = 0.5$. The arrow shows the direction of increasing Schmidt numbers. The dashed and solid lines show the spectra for the low wave numbers forcing and constant gradient forcing, respectively. The dashed-dotted line corresponds to the k^{-1} scaling under the chosen normalization.

$Sc = 0.7$ (Fig. 4 right). However, for $Sc = 0.7$ (the smallest Schmidt number value shown on figures), the spectrum does not exhibit a k^{-1} range (Fig. 4, left). This range is only found for $Sc > 1$, as predicted by theory.

Compared to previous studies and observations[8,32], our numerical results find the same behavior for the smallest scales. However, our numerical results clearly show a $-5/3$ inertial-convective range for this moderate Reynolds number, in constrast with previous works[7], where an imposed mean scalar gradient was used[8]. To better understand the influence of the forcing scheme at large and intermediate scales, additional simulations have been performed with an imposed mean scalar gradient to maintain the scalar variance. Figure 5 compares the scalar variance spectra for two Reynolds number, 130 and 210 and two Schmidt number, 0.7 and 4. The spectra are compensated by using the scaling of the inertial-convective range. As expected the small scales behavior is not influenced by the forcing schemes. But, for moderate Reynolds number, the influence of the forcing schemes clearly appears. The simulations using a mean scalar gradient forcing have no clear $k^{-5/3}$ range, and they have a

large k^{-1} range beginning at large scales. In particular, for $Sc = 0.7$, the scalar spectrum exhibits a viscous-convective range for the mean scalar gradient forcing, in contrast with the results obtained with a low wave numbers forcing and with the theoretical prediction. similar observations that have been made in previous results. As mentioned at the beginning of this letter, the results using mean gradient forcing reported by Donzis et al.[7] (see their figure 1 and 3) show also a k^{-1} range for $Sc < 1$ and no clear $k^{-5/3}$ range at $R_\lambda \approx 140$, whereas the results using a low wave number forcing reported by Watanabe and Gotoh[33] show a inertial convective range for similar Reynolds number (see their figure 4). Our numerical results suggest that these differences are due to the forcing scheme. When the Reynolds number increases, a inertial-convective range begins to appear for simulations with mean scalar gradient forcing, as shown by the spectra for $R_\lambda = 210$. Note that Watanabe and Gotoh[34] have already observed an influence of the forcing scheme on the scaling exponents of the structure function. However future works are needed to better understand how this forcing influence the spectrum behavior.

ACKNOWLEDGMENTS

This work is supported by the Agence Nationale pour la Recherche (ANR) under Contracts No. ANR-2010-JCJC-091601 and ANR-2010-COSI-009. This work was performed using HPC resources from GENCI-IDRIS (Grant 2012-020611). The authors thankfully acknowledge the hospitality of the Center for Turbulence Research, NASA-Ames and Stanford University, where part of this work has been done during the Summer Program 2012. The support of Institut Universitaire de France is gratefully acknowledged by the third author.

REFERENCES

[1]J.-B. Lagaert, G. Balarac, and G.-H. Cottet. Particle method: an efficient tool for direct numerical simulations of a high Schmidt number passive scalar in turbulent flow. *Proceeding of the CTR summer program, Stanford Univ.*, 2012.

[2]M. Lesieur. *Turbulence in fluids*. Fluid mechanics and its applications. Springer, Dordrecht, 2008.

[3]G. K. Batchelor. Small-scale variation of convected quantities like temperature in turbulent

fluid part 1. general discussion and the case of small conductivity. *J. Fluid Mech*, 5(01):113–133, 1959.

[4]S. Corrsin. On the spectrum of isotropic temperature fluctuations in an isotropic turbulence. *J. Appl. Phys.*, 22:469–473, 1951.

[5]A. M. Obukhov. The structure of the temperature field in a turbulent flow. *Dokl. Akad. Navk. SSSR*, 39:391, 1949.

[6]R. Kraichnan. Small-scale structure of a scalar field convected by turbulence. *Phys. Fluids*, 11:945–953, 1968.

[7]D. A. Donzis, K. R. Sreenivasan, and P. K. Yeung. The batchelor spectrum for mixing of passive scalars in isotropic turbulence. *Flow, Turbulence and Combustion*, 85:549–566, 2010.

[8]P K Yeung, Shuyi Xu, and K R Sreenivasan. Schmidt number effects on turbulent transport with uniform mean scalar gradient. *Physics of Fluids*, 14(12):4178, 2002.

[9]G.-H. Cottet, G. Balarac, and M. Coquerelle. Subgrid particle resolution for the turbulent transport of a passive scalar. In *Advances in Turbulence XII, Proceedings of the 12th EUROMECH European Turbulence Conference*, volume 132, pages 779–782, September 2009.

[10]A. Magni and G.H. Cottet. Accurate, non-oscillatory, remeshing schemes for particle methods. *Journal of Computational Physics*, 231(1):152 – 172, 2012.

[11]G.-H. Cottet and P. Koumoutsakos. *Vortex methods*. Cambridge University Press, 2000.

[12]P. Koumoutsakos and A. Leonard. High resolution simulation of an impulsively started cylinder using vortex methods. *J. Fluid Mech.*, 296, 1995.

[13]G.-H. Cottet and P. Poncet. Advances in direct numerical simulations of 3d wall-bounded flows by vortex-in-cell methods. *Journal of Computational Physics*, 193(1), 2004.

[14]P. Ploumhans, G.S. Winckelmans, J.K. Salmon, A. Leonard, and M.S. Warren. Vortex methods for direct numerical simulation of three-dimensional bluff body flows: Application to the sphere at re=300, 500 and 1000. *Journal of Computational Physics*, 178, 2002.

[15]P. Poncet. Topological aspects of the three-dimensional wake behind rotary oscillating circular cylinder. *J. Fluid Mech.*, 517, 2004.

[16]Georges-Henri Cottet, Bertrand Michaux, Sepand Ossia, and Geoffroy Vanderlinden. A comparison of spectral and vortex methods in three-dimensional incompressible flows. *J. Comput. Phys.*, 175(2):702–712, January 2002.

[17]W. M. van Rees, A. Leonard, D. I. Pullin, and P. K. Koumoutsakos. A comparison of vortex and pseudo-spectral methods for the simulation of periodic vortical flows at high reynolds numbers. *J. of Computational Physics*, 230:2794–2805, 2011.

[18]W.M. Van Ree, F. Hussain, and P. Koumoutsakos. Vortex tube reconnection at $re = 10^4$. *Physics of Fluids*, 24(7):75–105, 2012.

[19]S. E. Hieber and P. Koumoutsakos. A lagrangian particle level set method. *Journal of Computational Physics*, 210(1):342–367, 2005.

[20]M. Bergdorf and P. K. Koumoutsakos. A Lagrangian particle-wavelet method. *Multiscale Modeling and Simulation: A SIAM Interdisciplinary Journal*, 5:980–995, 2006.

[21]K. Alvelius. Random forcing of three-dimensional homogeneous turbulence. *Phys. Fluids*, 11:1880–1889, 1999.

[22]V. Eswaran and S. B. Pope. Direct numerical simulations of the turbulent mixing of a passive scalar. *Physics of Fluids*, 31(3):506–520, 1988.

[23]T. Gotoh, S. Hatanaka, and H. Miura. Spectral compact difference hybrid computation of passive scalar in isotropic turbulence. *Journal of Computational Physics*, 231(21):7398–7414, August 2012.

[24]C. da Silva and J. Pereira. Analysis of the gradient-diffusion hypothesis in large-eddy simulations based on transport equations. *Physics of Fluids*, 2007.

[25]D.A. Donzis and P.K. Yeung. Resolution effects and scaling in numerical simulations of passive scalar mixing in turbulence. *Physica D*, 239(14):1278–1287, July 2010.

[26]K.R. Sreenivasan. The passive scalar spectrum and the Obukhov–Corrsin constant. *Physics of Fluids*, 8:189, 1996.

[27]S.K. Lee, A. Benaissa, L. Djenidi, P. Lavoie, and R.A. Antonia. Scaling range of velocity and passive scalar spectra in grid turbulence. *Physics of Fluids*, 24:075101, 2012.

[28]L. Danaila and R.A. Antonia. Spectrum of a passive scalar in moderate Reynolds number homogeneous isotropic turbulence. *Physics of Fluids*, 21(11):111702, 2009.

[29]C. H. Gibson. Fine Structure of Scalar Fields Mixed by Turbulence. II. Spectral Theory. *Physics of Fluids*, 11(11):2316, 1968.

[30]D.I. Pullin and T.S. Lundgren. Axial motion and scalar transport in stretched spiral vortices. *Physics of Fluids*, 13(9):2553, 2001.

[31]D. Bogucki, H. Luo, and A. J. Domaradzki. Experimental evidence of the Kraichnan scalar spectrum at high reynolds numbers. *J. Phys. Ocean*, 2012. in press.

[32]D. Bogucki, A. J. Domaradzki, and P. K. Yeung. Direct numerical simulations of passive scalars with $Pr > 1$ advected by turbulent flow. *J. Fluid Mech.*, 343:111–130, 1997.

[33]T. Watanabe and T. Gotoh. Inertial-range intermittency and accuracy of direct numerical simulation for turbulence and passive scalar turbulence. *J. Fluid Mech*, 590:117–146, 2007.

[34]T. Watanabe and T. Gotoh. Intermittency in passive scalar turbulence under uniform mean scalar gradient. *Phys. Fluids*, 18(058105), 2006.